Implementation of 5G beamforming techniques on cylindrical arrays

Implementation of 5G beamforming techniques on cylindrical arrays

Daniel G. Riviello and Roberto Garello
Department of Electronics and Telecommunications (DET)
Politecnico di Torino
Torino, Italy
Email: {daniel.riviello, roberto.garello}@polito.it

***Abstract*—In this paper we study the performance of a Uniform Cylindrical Array for a 5G base station working in the mmW region. Conventional and Capon beamforming design are considered. A comparison against a base station equipped with three Uniform Planar Arrays, one per sector, is presented. Average per-user achievable rate results are provided with different system configuration in terms of network loading and number of antennas, showing that Uniform Cylindrical Array could represent an interesting solution for 5G mmW networks.**

***Index Terms*—Beamforming, cylindric arrays, planar arrays, 5G, mmW.**

I. Introduction

The growing demand for higher data rates in mobile communications will require new technologies able to offer increases in cellular capacity. The millimeter-wave (mmW) frequency spectrum is currently seen as a promising solution for achieving hundreds of times more capacity than current 4G cellular networks, and thus being considered for deployment in next generation 5G cellular systems [1].

Available bandwidths in the mmW frequency spectrum under 5G regulatory consideration (27 to 71 GHz) are much wider than todays cellular networks - up to 200 times greater than all current cellular allocations [2]–[4]. Furthermore, the small wavelengths will allow to implement massive MIMO techniques, array processing and beamforming (BF). However, larger communication impairments will be encountered at these frequencies, such as increased free space path loss, attenuation due to rainfall and other environmental factors, interference due to mutual coupling in the base station array etc., which can significantly increase the outage probability.

Array processing and BF design will play a key role in the future 5G mmW cellular networks. The larger number of antennas will facilitate not only compensation for the increased path loss, but also better management of the inter-user interference, thanks to advanced BF techniques, such as conventional and Minimum Variance Distortionless Response (MVDR) or Capon BF [9]. New massive MIMO and BF algorithms that resort to advanced signal processing techniques have been proposed for 5G [5]–[7], but most of them implement these algorithms on Uniform Linear Arrays (ULA's) or Uniform Planar Arrays (UPA's).

Base stations in 4G are usually equipped with with tri-sectorized (120° per sector) planar array antennas, which suffer from beam broadening and pattern degradation as the beam is steered toward azimuths or elevations angles far from broadside. Beam broadening might become an undesired feature in mmW 5G beamforming array systems, since it is required to have pencil beams for enhanced directivity in the azimuthal plane [4]. The compromise in directivity seriously affects the capability to distinguish multiple interferers, or in other words, the spatial resolution. On the other hand, conformal arrays, such as circular or cylindrical ones, have almost isotropic behavior, which means that the beam can be scanned in discrete steps through an arc while maintaining a constant pattern [8].

In this paper, we evaluate the performance of a 5G cellular network operating in the mmW region of the electromagnetic spectrum with a single base station (BS) equipped with an array of directive antennas capable of performing directional beamforming (both conventional BF and MVDR) towards the users of interest. We also resort to the stochastic geometry framework [10], [11], as single-antenna users are distributed according to an independent homogeneous Poisson point process in $\mathcal{R}^2$. We compare the scenario of a BS equipped with a Uniform Cylindrical Array (UCylA) of N total antennas and a BS with 3 UPA's, one per sector, each with $N/3$ antennas. The results are provided in terms of average per-user achievable rate with different system configuration (type of array, traffic loading, number of antennas).

The paper is organized as follows: Sec. II describes the system model, Sec. III illustrates the mathematical framework for cylindrical and planar arrays, in Sec. IV, the beamforming techniques and examples of array radiation patterns are presented. The results are shown and discussed in Sec. V and finally Sec. VI draws the conclusions.

II. System Model

Let us consider a circular cell of radius R in which K single-antenna users communicate with a Base Station (BS) located at the center of the circle, with height h from the ground equipped with an array of N antennas.

A. Spatial point process

Users are modeled as a spatial homogeneous Poisson point process with $h = 0$. Given a bounded area $\mathcal{A}$ of the plane, with $\mathcal{A} = \pi R^2$, the number of nodes of a point process existing in

the region $\mathcal{A} \subset \mathbb{R}^2$ is a random variable denoted by $M(\mathcal{A})$. The probability of K nodes existing in $\mathcal{A}$ is given by:

$$\Pr[M(\mathcal{A}) = K] = \frac{(\mu\mathcal{A})^K}{K!} e^{-\mu\mathcal{A}} \tag{1}$$

for an the average node density per unit area μ [nodes/km^2]. Since the process is homogeneous, μ is constant and location independent. Furthermore, given that there are K nodes of the Poisson process in $\mathcal{A}$, these points are conditionally independent and uniformly distributed in the circle. Hence, the locations of the randomly deployed K users have azimuth ϕ with uniform distribution between 0 and 2π and distance from BS ρ with the following probability density function:

$$f_\rho(\rho) = \frac{2\rho}{R^2}. \tag{2}$$

B. Baseband model

We focus on the uplink communication between K users and the BS . Let $\mathbf{x} = [x_1, x_2, \ldots, x_K]^T$ be the vector of symbols transmitted by the K users in a given time slot and carrier, each with power $E[|x_i|^2] = P_i$. Hence the baseband equivalent signal vector received by the N antennas at the BS is given by:

$$\mathbf{y} = \mathbf{H}\mathbf{x} + \mathbf{n} \tag{3}$$

where $\mathbf{H} = [\mathbf{h}_1, \mathbf{h}_2, \ldots, \mathbf{h}_K]$ represents the $N \times K$ wireless channel matrix, where each vector $\mathbf{h}_i \in \mathcal{C}^{N\times 1}$ represents the propagation channel vector from user i to the BS and $\mathbf{n} \sim \mathcal{CN}(0, \sigma_n^2\mathbf{I})$ is the spatially uncorrelated Gaussian noise vector. We consider in this paper a simplified channel model, suitable for mmW systems in wich the propagation is mostly Line of Sight (LOS) with a diffusive component [2], The channel vector for the i-th user is

$$\mathbf{h}_i = \sqrt{\gamma_i}\, \beta_i\, \mathbf{a}(\theta_i, \phi_i) \tag{4}$$

where the path loss γ_i is equal to:

$$\gamma_i = \left(\frac{\lambda}{4\,\pi\, d_i}\right)^2 \tag{5}$$

with d_i the distance of the i-th user from the BS and β_i is the Rician fading gain affecting the link between the i-th user and the BS with Rician factor F:

$$\beta_i \sim \mathcal{CN}\left(\sqrt{\frac{F}{F+1}}\, e^{j\xi},\ \frac{1}{F+1}\mathbf{I}\right) \tag{6}$$

with $\xi \sim \mathcal{U}(0, 2\pi)$. In addition, $\mathbf{a}(\theta_i, \phi_i)$ represents the steering vector (SV) or array response for the Direction of Arrival (DoA) of the i-th user with elevation angle θ_i and azimuth ϕ_i. In order to guarantee fairness among users, we adopt a simple power control mechanism and we assume that each user is assigned a transmit power P_i that is a fraction of the maximum transmit power P_{max} and compensates for the path loss:

$$P_i = \frac{d_i^2}{h^2 + R^2}\, P_{max} \tag{7}$$

We assume that decoding of the users' signals is performed at the BS with knowledge of both channel state information (CSI) and data signals and that the BS can obtain long-term averaged over the fading CSI for each user. For the sake of generality, the BS does not implement any scheduling strategy of the users, which communicate in the same time slot or resource, and the BS resorts only to Space Division Multiple Access (SDMA) through BF: for the case of a BS equipped with a UCylA, the interference of user i is made by the contribution of all remaining $K-1$ users, while for a BS with UPA's, interference for a user i in a specific sector will be generated only by the remaining users in the same sector. As final assumption, the BS is able to process all K users' signals, implying no limitation on the number of RF chains, i.e., the BS is able to employ at least K parallel beamformers.

The BS processes the K signals through the combining matrix $\mathbf{B} = [\mathbf{b}_1^H | \mathbf{b}_2^H | \ldots | \mathbf{b}_K^H] \in \mathcal{C}^{K\times N}$, where $\mathbf{b}_i$ is the $N \times 1$ beamformer or spatial filter designed for the i-th signal of interest with DoA (θ_i, ϕ_i), so that it attenuates all the other DoA's. The final estimated signal ensemble is given by

$$\hat{\mathbf{x}} = \mathbf{B}\mathbf{y} \tag{8}$$

with decision variable for the i-th user $\hat{x}_i = \mathbf{b}_i^h \mathbf{y}$. We can finally express the instantaneous Signal-to-Noise-plus-Interference ratio at decision variable $\hat{x}_i$ as:

$$SINR_i = \frac{P_i\, |\mathbf{b}_i^H \mathbf{h}_i|^2}{\sigma_n^2 |\mathbf{b}_i|^2 + \sum\limits_{\substack{k\in\mathcal{S} \\ k\neq i}} P_k |\mathbf{b}_i^H \mathbf{h}_k|^2} \tag{9}$$

where $\mathcal{S}$ is the whole set of K users when the BS is equipped with a cylindrical array, while $\mathcal{S}$ denotes the set of users within a sector for a BS with 3 sectorized planar arrays. The achievable rate for each user i is defined as:

$$C_i = \log_2(1 + SINR_i) \tag{10}$$

Results in this paper will be presented with the metric of the average per-user achievable rate

$$C = \mathrm{E}[C_i] \tag{11}$$

where expectation $\mathrm{E}[\cdot]$ is with respect to fading and users' positions.

III. Array processing

We will now describe how to express the array response or SV $\mathbf{a}(\theta_i, \phi_i)$ for a generic i-th user when the BS is equipped with 3 sectorized Uniform Planar Arrays (UPA's) or a Uniform Cylindrical Array (UCylA). We denote with N the total number of available antennas at the BS: for the UCylA $N_{\text{UCylA}} = N$, while for each of the 3 UPA's $N_{\text{UPA}} = N/3$. We assume the arrays are equipped with directive antenna elements, whose directivity function is of the kind:

$$D(\theta_i, \phi_i) = \begin{cases} u \sin\theta_i \cos(\phi_i - \delta) & \text{for } -90^\circ + \delta < \phi_i < 90^\circ + \delta \\ 0 & \text{otherwise} \end{cases} \tag{12}$$

where u is a scaling factor and δ the azimuthal direction to which the antenna element is pointed. We further assume perfect calibration of the arrays and no mutual coupling among the antenna elements.

A. Uniform Planar Arrays

We denote with $s = 0, 1, 2$ the sector index, the UPA with $s = 0$ lies on the yz-plane (broadside to $\theta = 90°$, $\phi = 0°$) with N_z antennas along z-axis and N_y along y-axis, $N_{\text{UPA}} = N_z N_y$, the UPA's with $s = 1$ and $s = 2$ have the same total number of elements and are broadside to ($\theta = 90°, \phi = 120°$) and ($\theta = 90°, \phi = 240°$) respectively. We can first write the $N_z \times 1$ SV of the Uniform Linear Array (ULA) on z-axis $\mathbf{a}_z(\theta_i)$ with element spacing $d_z = \lambda/2$ as

$$\mathbf{a}_z(\theta_i) = \left[1, e^{j\pi\cos\theta_i}, \ldots, e^{j\pi(N_z-1)\cos\theta_i}\right]^T \tag{13}$$

while we denote with $\mathbf{a}_y^{(s)}(\theta_i, \phi_i)$ the $N_y \times 1$ SV of the generic ULA that lies on the y-axis for $s = 0$ and it is rotated of $\pm 120°$ for $s \neq 0$ (with spacing $d_y = \lambda/2$):

$$\mathbf{a}_y^{(s)}(\theta_i, \phi_i) = \begin{bmatrix} 1 \\ e^{j\pi\sin\theta_i \sin\left(\phi_i - s\frac{2\pi}{3}\right)} \\ \vdots \\ e^{j\pi(N_y-1)\sin\theta_i \sin\left(\phi_i - s\frac{2\pi}{3}\right)} \end{bmatrix} \tag{14}$$

Finally, we can express the $N_{\text{UPA}} \times 1$ SV for each UPA as the Kronecker product of the 2 SV's along each axis multiplied by the element pattern:

$$\mathbf{a}_{\text{UPA}}^{(s)}(\theta_i, \phi_i) = u\sin\theta_i \cos\left(\phi_i - s\frac{2\pi}{3}\right)[\mathbf{a}_z(\theta_i, \phi_i) \otimes \mathbf{a}_y^{(s)}(\theta_i, \phi_i)] \tag{15}$$

B. Uniform Cylindrical Array

As for the planar case, we define a SV for a Uniform Cylindrical Array (UCylA). The array is made of N_z horizontal ring sub-arrays, spaced vertically at half wavelength, with N_u elements per ring. Each of these Uniform Circular Arrays (UCA's) has radius

$$r = \frac{\lambda N_u}{4\pi} \tag{16}$$

which guarantees $\lambda/2$ spacing on the circular arc between elements. As in the previous case, we can decouple the global array response of a UCylA into the Kronecker product of the SV of a UCA in the xy-place and the SV of a ULA lying in the z-axis. Let us first define the $N_u \times 1$ SV $\mathbf{a}_u(\theta_i, \phi_i)$ for the UCA with isotropic elements:

$$\mathbf{a}_u(\theta_i, \phi_i) = \begin{bmatrix} e^{j\frac{N_u}{2}\sin\theta_i\cos\phi_i} \\ e^{j\frac{N_u}{2}\sin\theta_i\cos\left(\phi_i - \frac{2\pi}{N_u}\right)} \\ \vdots \\ e^{j\frac{N_u}{2}\sin\theta_i\cos\left(\phi_i - 2\pi\frac{N_u-1}{N_u}\right)} \end{bmatrix} \tag{17}$$

and let us denote with $\mathbf{d}(\theta_i, \phi_i)$ the $N_u \times 1$ vector, which contains the values of the directivity function $D(\theta_i, \phi_i)$ associated with each element of the UCA:

$$\mathbf{d}(\theta_i, \phi_i) = \begin{bmatrix} u\sin\theta_i\cos\phi_i \\ u\sin\theta_i\cos\left(\phi_i - \frac{2\pi}{N_u}\right) \\ \vdots \\ u\sin\theta_i\cos\left(\phi_i - 2\pi\frac{N_u-1}{N_u}\right) \end{bmatrix} \tag{18}$$

It is easy to verify that, due to shadowing, half of the elements will be equal to zero in accordance with (12). The resulting $N_u \times 1$ SV of the UCA with directive antenna elements is equal to:

$$\mathbf{a}_{\text{UCA}}(\theta_i, \phi_i) = \mathbf{d}(\theta_i, \phi_i) \odot \mathbf{a}_u(\theta_i, \phi_i) \tag{19}$$

where $\odot$ denotes the Hadamard (entrywise) product.

Let us now define the $N_z \times 1$ SV of the ULA lying in the z-axis as:

$$\mathbf{a}_{\text{ULA}}(\theta_i) = \left[e^{-j\pi\frac{N_z-1}{2}\cos\theta_i}, \ldots, e^{j\pi\frac{N_z-1}{2}\cos\theta_i}\right]^T \tag{20}$$

where the difference with respect to (13) of the planar case is the phase reference point, which is the center of the cylinder. The global $N_{\text{UCylA}} \times 1$ SV of the UCylA finally becomes:

$$\mathbf{a}_{\text{UCylA}}(\theta_i, \phi_i) = \mathbf{a}_{\text{UCA}}(\theta_i, \phi_i) \otimes \mathbf{a}_{\text{ULA}}(\theta_i, \phi_i) \tag{21}$$

IV. Beamforming methods

We focus now on the design of the beamformer $\mathbf{b}_i$ design whose tasks are to correctly estimate the i-th signal of interest and attenuate interferers. Two different algorithms are taken into account for analysis:

1) Conventional BF,
2) Minimum Variance Distortionless Response (MVDR) BF or Capon BF.

A. Conventional beamforming

With this approach, also known as beam steering, the BS produces a phase shift to compensate for the delay of the DOA (θ_i, ϕ_i) for the i-th user, which is given by:

$$\mathbf{b}_i = \mathbf{a}(\theta_i, \phi_i). \tag{22}$$

B. MVDR beamforming

For MVDR BF, we first introduce the global spatial covariance matrix of noise plus interference for:

$$\mathbf{R} = \sigma_n^2\mathbf{I} + \sum_{k\in\mathcal{S}} P_k\,\gamma_k\,\mathbf{a}(\theta_k, \phi_k)\,\mathbf{a}^H(\theta_k, \phi_k) \tag{23}$$

where $\mathcal{S}$ is the set of user in the circle for UCylA and set of users in a sector for UPA's (one spatial covariance matrix per sector). Beamforming then becomes a constrained optimization problem that maximizes the power towards the i-th user of interest and minimizes the overall interference arising from other DoA's [9]:

$$\mathbf{b}_i = \frac{\mathbf{R}^{-1}\,\mathbf{a}(\theta_i, \phi_i)}{\mathbf{a}^H(\theta_i, \phi_i)\,\mathbf{R}^{-1}\,\mathbf{a}(\theta_i, \phi_i)} \tag{24}$$

C. Cylindrical and planar array patterns

We can define the the array gain function for any DoA (θ, ϕ) when the beamformer is designed for the DoA (θ_i, ϕ_i) of user i as:

$$\mathbf{G}(\theta, \phi\,|\,\theta_i, \phi_i) = |\mathbf{b}_i\,\mathbf{a}(\theta, \phi)|^2 \tag{25}$$

the array radiation pattern or array factor AF is equal to $AF(\theta, \phi\,|\,\theta_i, \phi_i) = \sqrt{\mathbf{G}(\theta, \phi\,|\,\theta_i, \phi_i)}$ and in the case conventional BF it has very well known expressions for linear, planar

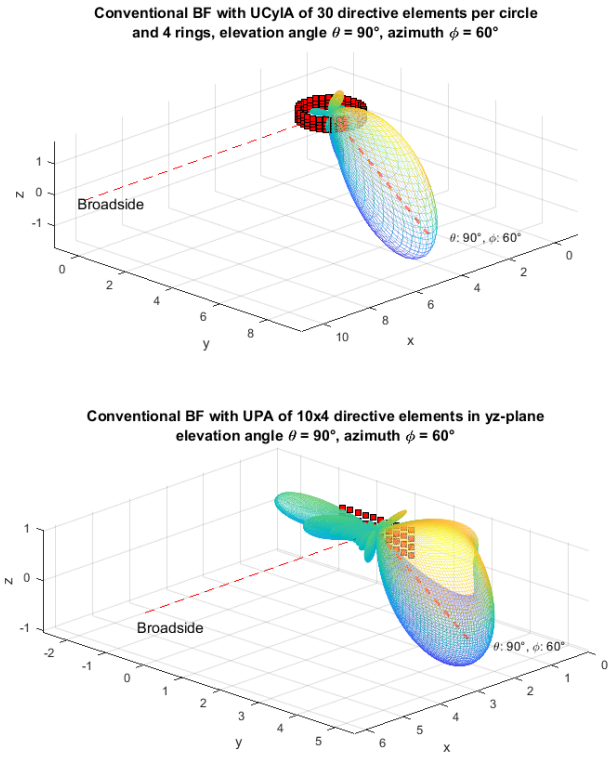

Fig. 1: Pattern with conventional BF for a 30×4 UCylA and a 10×4 UPA for DoA $(90°, 60°)$

[12], [13] and circular arrays [8]. For linear and planar arrays, beam broadening is a very well known feature that happens when the beam is steered toward azimuths or elevations angles far from broadside. Fig. 1 shows the radiation pattern with conventional BF for a DoA $(90°, 60°)$ of a UCylA with 4 rings along z and 30 directive element per ring on the top, and the radiation pattern of a UPA with 4 directive elements along z and 10 along y at the bottom. By focusing on the azimuthal plane, the beam remains constant for the UCA regardless of ϕ, while for ULA the beam broadening can be quantified in terms of Half Power Beamwidth $HPBW(\phi_0)$ for a generic azimuth ϕ_0 that can be approximated as $HPBW(\phi_i = \phi_0) \approx \frac{HPBW(\phi_i=0°)}{\cos\phi_0}$ [14]. In the next Section, we will try to evaluate and quantify how much beam broadening in UPA's affects the performance of the users in terms of achievable rate (i.e., SINR) w.r.t. to the UCylA.

V. Results

We compare now the performance of a BS equipped with a UCylA and 3 sectorized UPA's in terms of average-per-user rate with both conventional and MVDR BF. First, we summarize all simulation parameters in Tab. I

Fig. 2 shows the average per-user rate C as a function of the network load or user density μ, which ranges from 100 to 1000 users/km^2, or equivalently, an average number of users $\mathrm{E}(K) = \mu\mathcal{A}$ ranging from 12.6 to 125.7. It clearly confirms how MVDR is able to outperform conventional BF thanks

Parameter	Value
Radius of the cell R	200 m
Area of the cell $\mathcal{A}$	0.1257 km^2
Network load or user density μ	300 users/km^2
Carrier frequency f_c	28 GHz
Bandwidth B	100 MHz
Noise figure F	7 dBm
Maximum TX power P_{max}	20 dBm
Total antennas at UCylA N_{UCylA}	384
Total antennas per UPA N_{UPA}	128
Antennas along z for both arrays N_z	4
Antennas per ring (UCylA) N_u	96
Antennas along y (UPA) N_y	32
Directivity function $D(\theta_i, \phi_i)$	$2\sin\theta_i \cos(\phi_i - \delta)$
Height of the BS h	15 m
Rician factor F	10

TABLE I: Simulation parameters.

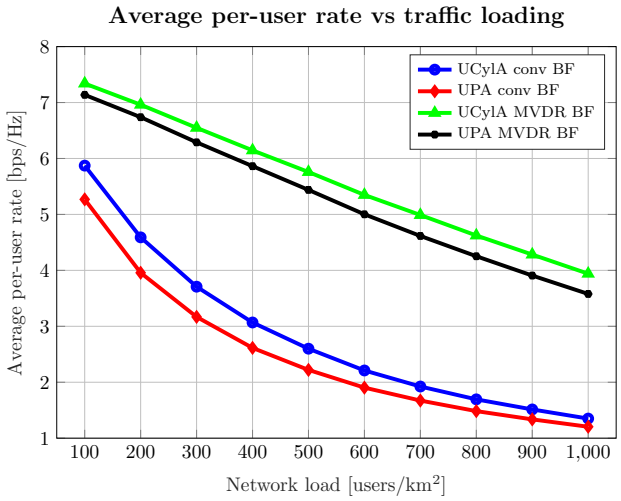

Fig. 2: Average per-user rate as a function of the network load (user density). Comparison between UCylA and 3 UPA's implementing both conventional and MVDR BF.

to its improved interference rejection capability, but it also shows that a BS equipped with a UCylA of 384 directive elements provides better average rate performance w.r.t. to 3 planar UPA's with each 128 directive antennas. The gap is almost 1 bps/Hz when the BS implements conventional BF for low network loads and it reduces with the increase in user density as well as the overall performance; for the MVDR BF case, the overall performance decreases more slowly (linear decrease) and the gap between UCylA and UPA is smaller, but it increases with network load.

Fig. 3 shows a polar plot in which the average per-user rate is plotted against the azimuthal DoA ϕ when conventional BF is adopted at the UCylA or the UPA's, while in Fig. 4

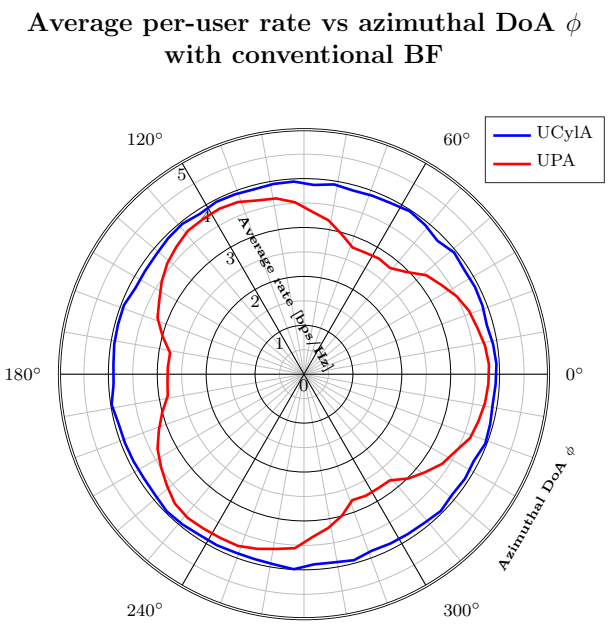

Fig. 3: Average per-user rate as a function of azimuthal DoA ϕ. Comparison between UCylA and 3 UPA's implementing both conventional BF, $\mu = 300$ users/km^2.

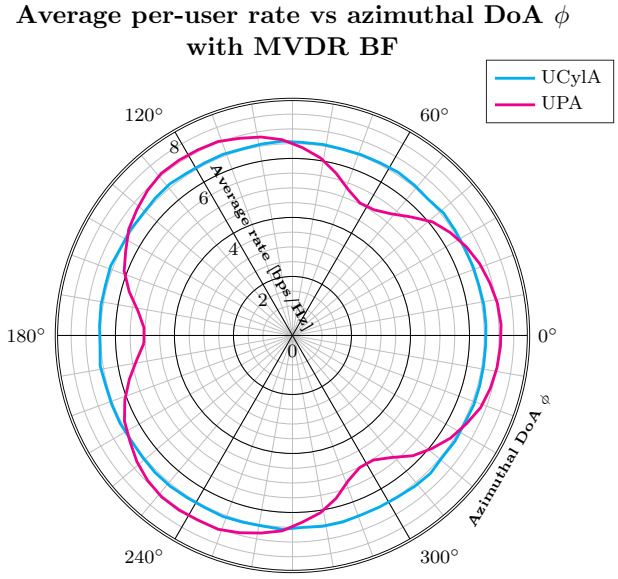

Fig. 4: Average per-user rate as a function of azimuthal DoA ϕ. Comparison between UCylA and 3 UPA's implementing both MVDR BF, $\mu = 300$ users/km^2.

MVDR BF is used. The UCylA exhibits uniform rate along all azimuths thanks to its isotropic behavior in both BF configurations; in Fig. 3 the 3 UPA's have slightly lower performance in those azimuthal regions that are broadside to the arrays, but the rate has clearly a significant reduction (more than 1 bps/Hz) for sector-edge users ($\pm 60°, 180°$), this is definitely caused by both beam broadening and directivity of the antenna elements which results in a reduce gain in sector-edge regions. Fig. 4 shows a similar polar pattern for the 3 UPA's in MVDR BF configuration, in this case the UPA's are able to outperform the UCylA in the broadside region (0.5 bps/Hz above UCylA), but users in sector-edge region suffer a more pronounced decrease in performance (1.5 bps/Hz below UCylA). It is finally worth noticing that MVDR BF can offer more than 1.5 times better achievable rate performance w.r.t. to conventional BF.

VI. Conclusions

The performance of a 5G Base Station equipped with a Uniform Cylindrical Array and working in the mmW region has been evaluated and compared with a Base Station equipped with 3 sectorized Uniform Planar Arrays. Conventional and Capon beamforming have been considered. The results, presented in the form of achievable average per-user rate and provided with different configurations, have confirmed the improved interference rejection capability of the MVDR technique, but have also shown that cylindrical arrays exhibit better performance w.r.t. to planar arrays, and especially a uniform rate distribution along the azimuthal users' direction of arrival. Cylindrical arrays could thus represent an interesting solution for 5G mmW networks.

References

[1] W. Roh, J. Seol, J. Park, B. Lee, J. Lee, Y. Kim, J. Cho, K. Cheun and F. Aryanfar, "Millimeter-wave beamforming as an enabling technology for 5G cellular communications: theoretical feasibility and prototype results," *IEEE Communications Mag.*, pp. 106-113, Feb. 2014.

[2] M. R. Akdeniz, Y. Liu, M. K. Samimi, S. Sun, S. Rangan, T. S. Rappaport and E. Erkip, "Millimeter Wave Channel Modeling and Cellular Capacity Evaluation", *IEEE Journal on Selected Areas in Communications*, vol. 32, no. 6, pp. 1164-1179, June 2014.

[3] T. S. Rappaport, W. Roh, and K. Cheun, "Mobiles millimeter-wave makeover," *IEEE Spectrum*, pp. 35-56, Sep. 2014.

[4] S. Han, C. Lin, Z. Xu, and C. Rowell, "Large-scale antenna systems with hybrid analog and digital beamforming for millimeter wave 5G," *IEEE Communications Mag.*, pp. 186-194, Jan. 2015.

[5] R. W. Heath, N. Gonzlez-Prelcic, S. Rangan, W. Roh and A. M. Sayeed, "An Overview of Signal Processing Techniques for Millimeter Wave MIMO Systems," in *IEEE Journal of Selected Topics in Signal Processing*, vol. 10, no. 3, pp. 436-453, Apr. 2016.

[6] O. E. Ayach, S. Rajagopal, S. Abu-Surra, Z. Pi and R. W. Heath, "Spatially Sparse Precoding in Millimeter Wave MIMO Systems," in *IEEE Transactions on Wireless Communications*, vol. 13, no. 3, pp. 1499-1513, Mar. 2014.

[7] A. Alkhateeb, J. Mo, N. Gonzalez-Prelcic and R. W. Heath, "MIMO Precoding and Combining Solutions for Millimeter-Wave Systems," in *IEEE Communications Magazine*, vol. 52, no. 12, pp. 122-131, Dec. 2014.

[8] L. Josefsson and P. Persson, *Conformal Array Antenna Theory and Design*, John Wiley, Hoboken, NJ, Chapter 6, 2006.

[9] J. Capon, "High-Resolution Frequency-Wavenumber Spectrum Analysis," *Proceedings of the IEEE*, vol. 57, no. 8, pp. 1408-1418, Aug. 1969.

[10] M. Haenggi, "On distances in uniformly random networks", *IEEE Transactions on Information Theory*, vol. 51, no. 10, pp. 3584-3586, Oct. 2005.

[11] S. Srinivasa and M. Haenggi, "Distance Distributions in Finite Uniformly Random Networks: Theory and Applications", *IEEE Transactions on Vehicular Technology*, vol. 59, no. 2, pp. 940-949, Feb. 2010.

[12] Balanis, Constantine A, *Antenna theory: analysis and design*, Wiley-Interscience, 2005.

[13] Harry L. Van Trees, *Optimum Array Processing: Part IV of Detection, Estimation, and Modulation Theory*, John Wiley & Sons, 2004.
[14] Hubregt J. Visser, *Array And Phased Array Antenna Basics*, John Wiley & Sons Inc, 2005.